COMPARISON OF RESULTS FROM LOW-GRAVITY AND NORMAL GRAVITY EXPERIMENT "TRACE" ON THE COLUMNAR-EQUIAXED TRANSITION IN THE TRANSPARENT ALLOY SYSTEM NEOPENTYLGLYCOL-CAMPHOR

Laszlo Sturz, Gerhard Zimmermann

ACCESS e.V., Intzestrasse 5, 52072 Aachen, Germany, Email: L.Sturz@access-technology.de

ABSTRACT

In 2009 the experiment "TRACE" (TRansparent Alloys in Columnar Equiaxed solidification) has been carried out onboard the sounding rocket TEXUS-47 in low-gravity environment. The experiment aimed at investigating the transition from columnar to equiaxed dendritic growth during solidification of the transparent organic alloy system Neopentylglycol (NPG)-(D)Camphor (DC). The transition was observed in-situ and real-time in a transparent cell. For the first time all relevant experimental parameters like thermal gradient, solidification velocity and undercooling within the bulk liquid and at the columnar dendritic tips have been determined directly from the experiment.
Here we present a summary of some of the experimental results including a comparison to the reference experiment carried out under terrestrial gravity conditions. The results serve as precise benchmark data for a comparison with theoretical models and numerical simulations on the columnar-equiaxed transition.

1. INTRODUCTION

Solidification of a molten alloy system is often accompanied by the formation of dendritic microstructures at the propagating solid-liquid interface or in the melt pool. These dendrites may undergo coarsening or phase transformations upon further cooling towards the final microstructure at ambient. Nevertheless, the first microstructure formation from the liquid is of fundamental importance for the mechanical properties of the solidified specimen.
The columnar-to equiaxed transition (CET) is related to a change in microstructural and thus mechanical features of this primary phase. As a simplified rule-of-thumb columnar dendritic growth is obtained at high thermal gradients and low cooling rates at the dendritic interface between solid dendrites and liquid melt and equiaxed dendritic growth vice versa. Neighbouring dendrites having the same crystallographic orientation are organized in grains within a dendritic network. These columnar grains, as well as the constitutive dendrites have elongated shapes, and are oriented towards the temperature gradient direction. A misorientation of the grains against the gradient direction may occur, depending for example on the anisotropy level of the solid-liquid interface energy. The dendrite tips at the front within a grain grow at the same level of undercooling, compared to the equilibrium liquidus-temperature of the alloy, indicated in the phase-diagram (Fig. 1). Columnar dendritic growth is favoured for example in single crystal growth [1] or in some turbine blades [2]. Equiaxed grain structures show more isotropic properties and are formed upon nucleation and growth. Generally, these structures have smaller grain sizes with shape factors closer to one and random crystallographic orientations. A mixed columnar-equiaxed structure with a transition zone (the CET) is in general undesirable for a technical product, since microstructural changes can lead to heterogeneities in its' mechanical properties. Experiments with forced transitions are thus aimed to investigate the conditions and physical mechanisms at the CET to improve predictions for stable processing windows.
A sufficiently undercooled bulk region at the dendritic front has to be established during solidification for the occurrence of CET. Size of this constitutionally undercooled zone and level of undercooling are related to thermodynamical, thermophysical and experimental parameters [3,4].
Dendritic fragments can be detached from the growing columnar network by mechanical shear stress or due to re-melting of dendritic necks [4]. Transportation of these fragments into the undercooled melt for example by buoyancy forces, can lead to growth of an equiaxed zone [5]. Equiaxed dendrites may also form by heterogeneous nucleation of the primary phase on substrates or impurities. If the equiaxed grains ahead the columnar dendrites are sufficient in volume fraction, they can block the columnar growth front and result in CET. The origin of equiaxed grains, the conditions, criteria and physical mechanisms responsible for CET and the effect of gravity are topics of active research. In general, gravity can act as a driving force for natural (thermo-solutal) convection in addition to the diffusive transport of mass and heat and

Proc. '20th ESA Symposium on European Rocket and Balloon Programmes and Related Research'
Hyère, France, 22–26 May 2011 (ESA SP-700, October 2011)

can initiate sedimentation/buoyancy of solid particles/grains. These gravity effects depend also on the size of the particles/grains and the geometry of the solidification volume. In low-gravity conditions like in sounding rockets the CET-phenomenon is reduced to a few processing and alloy parameters, which can be tackled by numerical or analytical descriptions.

Here, we present a comparison between a CET-experiment carried out under low-gravity conditions and the corresponding reference experiment on ground. The microgravity experiment was carried out on the sounding-rocket mission TEXUS-47 in 2009. An optically transparent organic alloy material is used, in which columnar dendritic growth and the CET can be observed within a glass cell by standard optical techniques in-situ and real-time. Details of the experimental preparation and procedure will be given in section 2, while the results will be summarized in section 3.

2. EXPERIMENTAL PART

2.1. Alloy preparation and properties

The organic materials (2,2-Dimethyl-1,3-propanediol; Neopentylglycol=NPG; CAS-no. 126-30-7 and (1R)-(+)-Camphor=DC; CAS-no. 464-49-3) have been purchased in commercial purity, i.e. 99% NPG and 98% DC. They have been purified twice by sublimation and re-condensation at a pressure of about 10^{-3} bar. The complete handling of the materials was carried out under argon atmosphere (ARG 6.0) at ambient pressure in a sealed glove-box. The final products have been analysed using gas chromatography-mass spectrometry (GC-MS) to obtain less than 0.3 wt% of residual organic material remaining in DC, while no contamination could be measured in NPG. The GC-MS procedure excludes the detection of dissolved gases and water. The products have been alloyed as NPG-37.5 wt.-%DC from the mixed purified solid materials in a sealed glass-bottle containing argon by heating above their common liquidus-temperature. The homogenized liquid alloy is then sucked into a gas-tight glass-syringe, which is sealed afterwards for further use.

Fig. 1 shows the binary phase-diagram of the NPG-DC system, taken from [6]. The following characteristic equilibrium temperatures are obtained for the NPG-37.5 wt.-%DC alloy from the phase-diagram: solidus (eutectic)-temperature T_S=54±1°C, solid state transformation (i.e. fcc-monoclinic) temperature T_{SS}=40±1°C. The liquidus-temperature is measured in-situ in a thermal-gradient after equilibration and is obtained to be T_L=64±1°C. The solidification range is thus 10°C. During directional solidification all transformation temperatures may be subject to some level of undercooling. A summary of some other relevant alloy properties is given in Tab. 1.

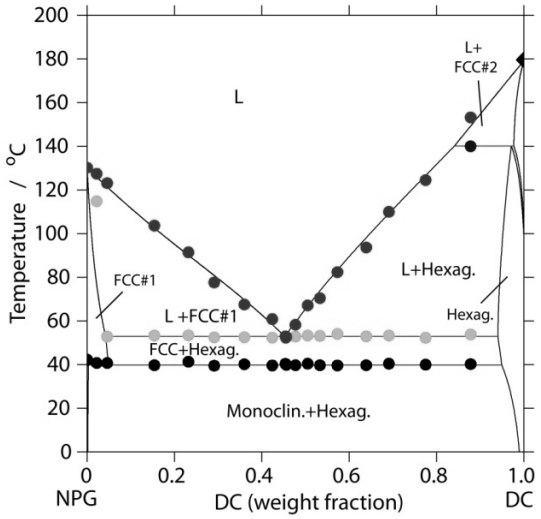

Figure 1: Phase-diagram of NPG-DC. Alloy chosen is NPG-0.375 wt.-fraction DC.

Table 1: Some thermodynamic and thermophysical properties of NPG-37.5wt.-%DC alloy.

Property	Value
liquidus-slope m_L	-1.65 K/wt%[(a)]
partition-coeff. k	0.086[(b)]
diffusion coefficient in liquid D_L	$5.2*10^{-11} \leq D_L \leq 7.0*10^{-11}$ m^2s^{-1}[(c)]
Gibbs-Thomson-coefficient Γ	$7.8*10^{-8}$ Km[(d)]
latent heat L	$3.34*10^4$ Jkg^{-1}[(e)]
heat of transformation	$7.18*10^4$ Jkg^{-1}[(f)]

(a): linear fit from phase-diagram in the hypoeutectic range, see Fig. 1; (b) averaged between T_S and T_L, deviations are ≤ 0.004; (c): from planar-cellular-transition in NPG-17wt%DC; (d): weighted average between Γ=(8.58±0.96)*10^{-8} Km (Camphene, [7]) and Γ=(7.4±0.7)*10^{-8} Km (Neopentylglycol, [8]); (e): from thermo-dynamic CALPHAD-description [6]; (f): from thermodynamic CALPHAD-description [6], solid-state-transformation at 40°C.

2.2. Experimental set-up and procedure

The experimental set-up is based on previously used hardware-developments for sounding rockets investigating planar and cellular growth in transparent model alloys [9-10]. For the experiment "TRACE" on TEXUS-47 the experimental volume was contained in between a steel frame and two quartz-glass plates. The steel frame size is 20 mm in width, 16 mm in height and 1 mm in thickness. Within the frame a bottom inlet and top outlet supports feeding of the liquid alloy and volume compensation during thermal and phase-change shrinkage and expansion. Five holes at one side of the frame allowed for the insertion of thermocouples to follow the temperature evolution during the experiment. Two quartz-glass plates of 4 mm thickness sealed the experimental volume at the main sides. A

schematic drawing of the set-up is given in Fig. 2. The experimental volume was illuminated from one side with monochromatic LED-light and observed with two different optical systems: A beam splitter provided a microscopic observation of solidification details within a field-of-view of 2.1 mm width and 1.7 mm height, while in parallel an overview image with field-of-view of 25 mm width and 18.3 mm height was acquired.

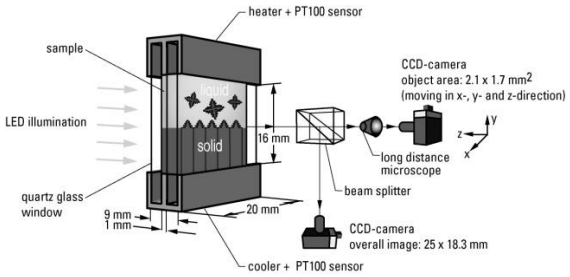

Figure 2: Schematic simplified drawing of the main parts of the experimental set-up.

Five thermocouples type K of 0.25 mm diameter were inserted from one side within the experimental volume at position 3.2 mm, 5.7 mm, 8.2 mm, 10.8 mm and 13.1 mm, measured from the bottom of the experimental volume with an estimated precision of ±0.1 mm. The points of temperature measurements within the thermocouples were located at 2.5±0.2 mm distance from the edge of the cell. The acquisition rate of the thermocouples was 10 Hz. Due to the small size of the thermocouples, their lateral insertion and position we do not expect the thermocouples to influence the thermal field or the nucleation events.

The experiment was controlled at some distance from the bottom with a peltier cooler and at some distance from the top by a resistance heater, both using PT-100 temperature sensors. Melting and solidification was controlled by these temperatures only, there were no moving parts like in classical Bridgman-experiments. The alloy-containing syringe was connected to the experimental cell via an inert steel tube. The cell was filled with the molten alloy material in the pre-heated syringe without bubbles and allowed for fast solidification to avoid segregation effects upon first freezing.

Tab. 2 summarizes the experimental procedure for "TRACE". Before lift-off the cell was oriented vertically upwards in the payload. The images of both of the cameras, as well as the house-keeping data and thermal data from the thermocouples were transmitted during the complete experimental run on ground and during flight, except small time-intervals after lift-off and re-entry of the rocket and very rare telemetry malfunctions. The corresponding reference-experiment on ground was carried out with the identical experimental procedure as given in Tab. 2 with solidification vertically upwards during the complete experiment.

The CET is provoked externally by increasing the cooling-rate at both the cooler and the heater by a factor of 10. Following parameters were obtained from the experiments as functions of experimental time and are summarized here: (i) gravity level, (ii) equiaxed dendrite density, (iii) equiaxed, columnar and liquid volume fraction, (iv) thermal gradient, (v) columnar front position, velocity and undercooling.

Table 2: Experimental procedure for the low-gravity experiment. The time refers to lift-off of the sounding-rocket at t=0 s.

Time	Action
≅- 4h30 min.	Complete melting of the alloy from RT. T_H=90°C, T_C=80°C.
≅- 4h15 min.	Thermal mixing by convection. T_H ≅65°C, T_C =80°C.
≅- 1h30 min.	Uncontrolled nucleation and solidification from bottom, T_H =90°C, T_C =50°C.
≅- 1h10 min.	Columnar dendritic growth due to bottom cooling at -0.2 $Kmin^{-1}$.
≅- 40 min.	Columnar dendritic growth due to both bottom and top cooling at -0.2 $Kmin^{-1}$.
0 s.	Rocket lift-off, high accelerations.
<+ 60 s.	Burn-out of rocket stages, de-spinning and stabilization of rocket.
+ 60 s.	Gravity level < 1 mg.
+ 60 s.	Initiation of CET: Cooling-rate increase from -0.2 $Kmin^{-1}$ to -2.0 $Kmin^{-1}$.
+ 480 s.	Re-entry of rocket, end of low-gravity period.

T_H: Heater temperature, T_C: Cooler temperature, RT=room temperature.

3. RESULTS AND DISCUSSIONS

3.1. Gravity level

The gravity level was measured within the payload of the TEXUS-47 rocket along three axes (one along the rocket axis). During the rocket ascent accelerations up to 13 g were measured, while the gravity level dropped below ±1 mg for all axes at about 60 s and kept at this level for roughly the first half of the experiment with the exception of a few spikes up to ±2 mg. In the second half a slight continuous increase up to ±4 mg was observed till the re-entry of the rocket into atmosphere with de-accelerations up to 18 g.

3.2. CCD-images

Fig. 3 shows a sequence of overall CCD-images obtained from the "TRACE"-experiment at selected time-steps (Fig. 3a+b) and the reference experiment

(Fig. 3c). The five thermocouples are visible on the left-hand side and the outlet at the top of the cell. Focused microstructures are obtained with an optical resolution of about 30 µm in the image-plane. Within the sheet-like cell of 1 mm depth 1-3 dendritic columns can be observed (in the detail image, which allow for focal change) at different depth positions behind each other. In the first image at *t*=-4min42s before lift-off columnar dendritic growth can be observed with the dendrites' organized in differently tilted grains against the thermal gradient direction (vertically upwards). Close to the lowest thermocouple at *z*=3.2 mm from the bottom of the cell the eutectic front is growing (dark contrast). In the second image at *t*=+7min15s after lift-off equiaxed dendrites can be observed with different sizes and extending from the columnar front up to roughly 2.0 mm into the liquid. Some equiaxed dendrites have been engulfed in the growing columnar front already, and the columnar front is arrested by the equiaxed dendrites (CET). In the last image from the reference experiment at *t*=+6min30s after (virtual) lift-off we have the CET under 1 g conditions.

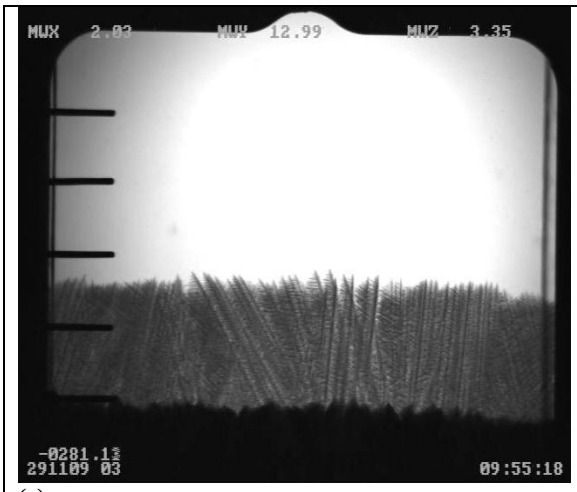

(a)

(b)

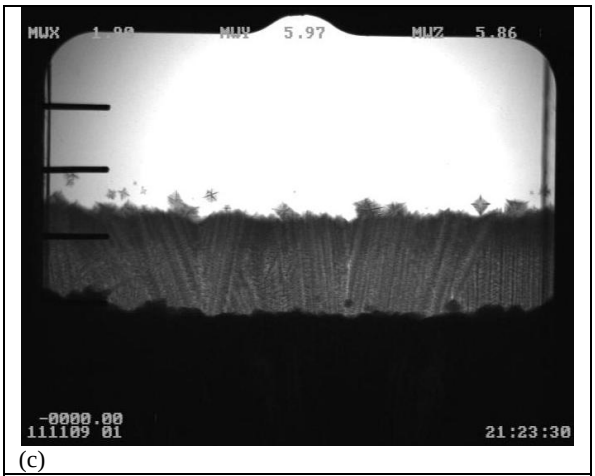

(c)

Figure 3: Selected overall CCD-images (a) at -4min42s and (b) +7min15s relative to rocket lift-off. (c): at +6min30s in the reference experiment.

3.3. Nucleation process and equiaxed grain density

Due to in-situ observation as shown in Fig. 3 it was concluded, that no fragmentation of dendrite arms from the columnar front was responsible for nucleation events. Heterogeneous nucleation on suitable substrates is the nucleation mechanism. The chemistry of the substrate is unknown, but we recall the existence of remaining organic impurities in DC (sec. 2.1) and inorganic impurities like dust can also not be avoided completely. It was observed (for example see Fig. 3b), that the equiaxed dendrites nucleated at different axial positions within the temperature field. The corresponding nucleation temperatures are within a certain range, which could be attributed to either substrates of different size or type.

We determined the number-density of equiaxed dendrites in time. The volume of analysis extends from the lowest visible liquid area in the columnar front into the liquid up to the uppermost visible equiaxed dendrite. We recall that the optical resolution in the observation plane is about 30 µm, thus dendrites/nuclei of smaller size cannot be detected or observed. Equiaxed dendrites engulfed into the growing columnar front with more than 50 area% were not taken into account. Fig. 4 shows the result for equiaxed dendrite density for "TRACE" and the reference experiment.

We observe a continuous increase of the density in both experiments up to 0.5 grains per mm^3 in "TRACE" and 0.7 grains per mm^3 in the reference experiment, respectively. At the end of the microgravity period the density has not reached a steady-state in both cases. The development of equiaxed grains is delayed in "TRACE".

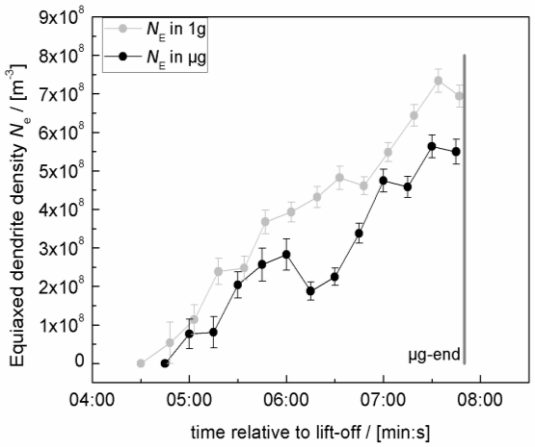

Fig. 4: Equiaxed grain density as function of experimental time. Error bars correspond to a counting error of ±1 grain.

3.4. Equiaxed volume fraction

The increase in volume fraction of equiaxed grains was analysed for comparison with theoretical predictions. In 1984, Hunt [11] proposed a criterion with regard to the equiaxed volume fraction ϕ_E, later called "mechanical blocking criterion". Following Hunt, at $\phi_E \geq 0.49$ equiaxed growth is obtained and columnar growth for $\phi_E \leq 0.0066$ (1% of "extended" equiaxed fraction, [11]). A mixed columnar-equiaxed region exists in between these values. The value of $\phi_E \geq 0.49$ corresponds to a shape factor smaller or equal than 2 for equiaxed growth. The critical value in equiaxed volume fraction was discussed critically by Biscuola et al. [12] and the authors propose a lower mechanical blocking criterion of $\phi_E=0.20$ due to better agreement with cellular automata simulations in AlSi7 [12].

Here, the equiaxed volume fraction is determined within a rectangular box volume as a function of time. The height of the box volume extends from the lowest visible liquid area at the columnar front into the liquid up to 0.5 mm ahead of the foremost dendrite tip. This assumed value corresponds to the maximum primary dendrite arm spacing PDAS in columnar growth found experimentally. Width and depth of the box correspond to the cell boundaries (20 mm x 1 mm). Since the depth remains constant, we calculate to area fractions rather than volume fractions. The individual equiaxed dendrite area was estimated by the area of a fitted ellipse, enveloping the dendrite tips. The total equiaxed area is the sum of all ellipse areas. Equiaxed dendrites engulfed for more than 50 area% into the columnar front are defined as part of the columnar area. All equiaxed dendrites with centres outside the box volume are not accounted for. The columnar area is determined as the area within the lower box edge and the columnar front envelope. An example for the box, the columnar area and one equiaxed dendrite with elliptical circumference is shown in Fig. 5.

The liquid area fraction ϕ_L is calculated by $\phi_L=1-\phi_E-\phi_C$, where ϕ_E is the total equiaxed area fraction and ϕ_C the columnar area fraction. Fig. 6 shows the calculated fractions as function of time for "TRACE" and the corresponding reference experiment. As can be seen, the equiaxed volume fraction increases upon nucleation and growth and approaches a plateau within the available microgravity time. The plateau is more pronounced for the reference experiment and starts at +6min30s after (virtual) lift-off with a plateau value of $\phi_E=0.20$-0.26. Within "TRACE" a first plateau is reached at +6min30s with a value of about $\phi_E=0.17$, but a further increase to $\phi_E=0.36$ is found at +7min15s after lift-off. In both cases the columnar fraction remains more or less constant, while the liquid fraction decreases due to the increase in equiaxed volume fraction. The small difference between the two experiments cannot be attributed solely to gravity, since the statistics are not sufficient.

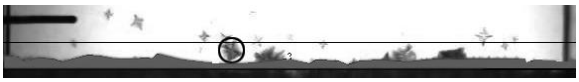

Figure 5: Example for box, columnar front envelope and area (shaded grey) and one equiaxed dendrite with elliptical circumference for calculation of the different volume fractions: equiaxed, columnar and liquid.

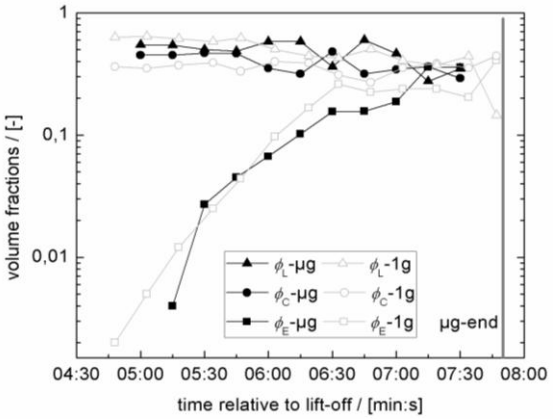

Figure 6: Evolution of volume fractions of liquid, columnar and equiaxed in "TRACE" and the corresponding reference experiment.

In both cases the CET is obtained and we define the time at CET through the volume fractions and the corresponding images. Thus CET occurs at +6min30s and at +7min15s in the reference and the low-gravity experiment, respectively. This corresponds to images Fig. 3b+3c. Again, as in the equiaxed grain density, the CET is delayed in "TRACE". The corresponding values of $\phi_E=0.23$ (in average) and $\phi_E=0.36$ are within

some limits related to the definition of the box height. Nevertheless a deviation from the ϕ_E=0.49 criterion [11], towards ϕ_E=0.20 [12] can be observed.

3.5. Thermal data

Fig. 7 shows the temperature evolution at the control points (T_H, T_C) in the heater and the cooler and the cooling curves measured at the five thermocouples T1 to T5 for "TRACE". Some errors exist due to telemetry malfunctions at about -2200 s and +300 s. The curves show the onset of the low cooling-rate -0.2 Kmin^{-1}, the increase to -2.0 Kmin^{-1} at t=60 s and the thermal reaction of the system at the thermocouples.

Fig. 8 shows the thermal gradient obtained from the cooling curves (and the position of the columnar front) by several methods. Method "T1-T5" calculates the temperature difference between T1 and T5, divided by their distance of 9.9 mm (sec. 2.1). Within this method the gradient is averaged over the different phases of the alloy (liquid, mushy-zone, eutectic) with changing fractions in time and over large length scales without resolving local events. Method "G_L" calculates the thermal gradient more locally ahead of the liquidus-temperature by the temperature difference (from measured liquidus-temperature) to the next thermocouple, divided by the distance of the thermocouples. Method "G_F" is similar to method "G_L", but relies on the calculation of the thermal gradient ahead of the columnar front towards the next thermocouple. Hence the undercooling of the columnar front below the liquidus-temperature is taken into account.

In general, all methods result in values for the thermal gradients between 16 and 19 Kcm^{-1} in the relevant experimental sections with applied cooling rates. Method "G_F" gives unsystematic errors due to the error (averaging) in the determination of the front position (sec. 3.6). The methods "G_L" and "T1-T5" give similar values at the beginning (<3000 s), when most of the cell consists of liquid phase. With increasing fraction of solid, method "T1-T5" results in lower values (difference of 0.5-1.0 Kcm^{-1}) for the thermal gradient, when compared to "G_L". This is due to different thermal conductivities λ in liquid "L" and solid "S" with λ_S<λ_L. The differences between "TRACE" and the reference experiment are within 5% in the relevant experimental sections and for methods "G_L" and "T1-T5". At the CET (sec. 3.4) the values are 17.0±1.0 Kcm^{-1} and 16.5±1.0 Kcm^{-1} for the reference experiment and for "TRACE", respectively. Here the difference in the methods is accounted for in the error-values.

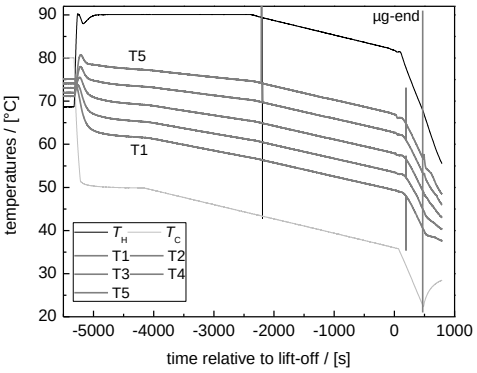

Figure 7: Temperature evolution inside the experimental cell and at cooler and heater.

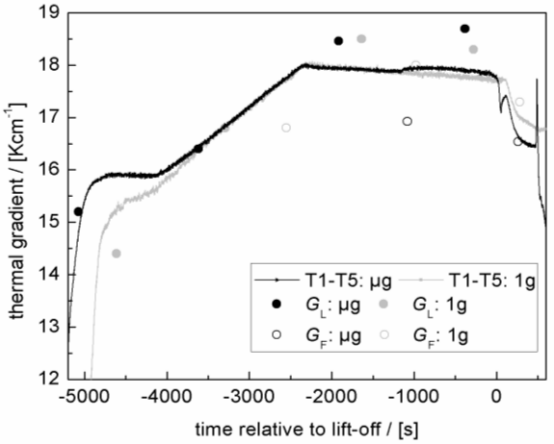

Figure 8: Temperature gradient obtained for three different methods (see text).

3.6. Front position, velocity and temperature

The front-position is obtained by automatic image processing from the CCD-images at 10 different lateral equidistant positions, see Fig. 9. The leftmost and rightmost positions were not taken into account; neither were those lines in Fig. 9 crossing equiaxed structures. The remaining positions are averaged and the average curves are shown in Fig. 10a. The front-velocities are derived from the derivatives of the front-positions and shown in Fig. 10b. The front-temperatures are derived from the front positions and linear interpolation of the measured temperatures for the two thermocouples below and above the front. The front undercooling in both cases is calculated form the difference of the front-temperature to the liquidus-temperature of T_L=64±1°C and shown in Fig. 10c.

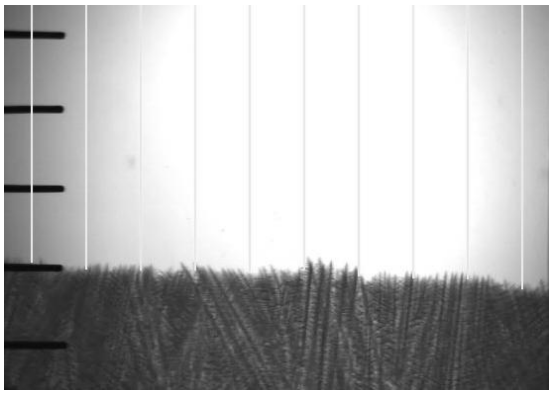

Figure 9: Determination of front-position.

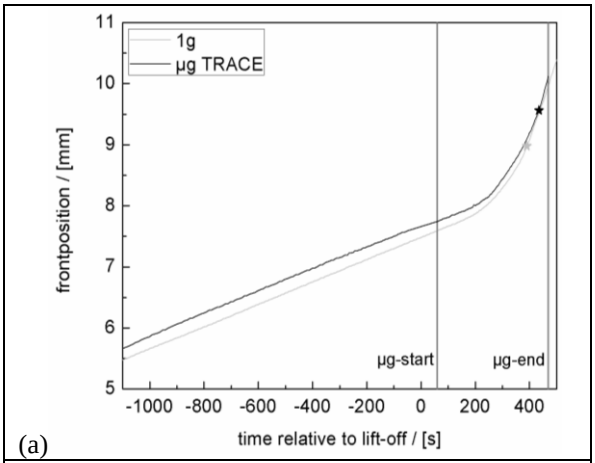

(a)

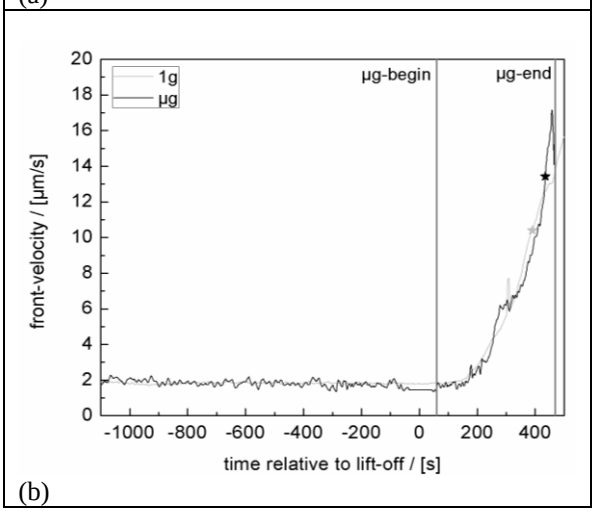

(b)

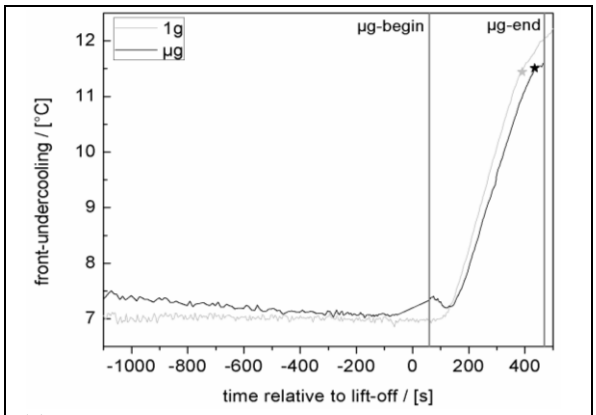

(c)

Figure 10a-c: Averaged positions, velocities and undercoolings of the front.

In all cases the curves are close to each other. There is an artefact due to changing the power-supply in the TRACE experiment at about -100 s, which leads to a restabilisation of the system and to the "humb" in Fig. 10c from -100 s to +100 s. As a small tendency, the CET seems to be accelerated a little bit in the 1g-experiments, concerning the critical values for position, velocity and undercooling of the front. This tendency was already observed in the number-density and the volume fraction of equiaxed grains.

4. SUMMARY AND CONCLUSIONS

The columnar-to-equiaxed transition in dendritic solidification was investigated in the organic transparent alloy system NPG-37.5wt.-%DC. The experiments have been carried out on the sounding-rocket TEXUS-47 in 2009, as well as on ground with identical parameters. The CET was provoked here by increasing the cooling rate by a factor of 10.

The results reported here can be summarized as follows:

- The gravity level in the low-gravity period during "TRACE" was lower than ±4 mg in all directions,
- During the low-gravity period (+60 s to +470 s) the CET occurred at +390 s in the reference experiment and at +435 s in the low-gravity experiment "TRACE",
- As a small tendency, the CET is accelerated in the 1g-experiments,
- The differences between the low-gravity and the reference experiment are small, mainly due to the small depth of the experimental volume, the (critical) values at the CET can be summarized as:

	"TRACE"	1g-reference
Time	7:15 min. after "LO"	6:30 min. after "LO"
Front undercooling	11.5°C	11.4°C
Front velocity	13.5 μms^{-1}	10.5 μms^{-1}
Thermal gradient	16.5 Kcm^{-1}	17.0 Kcm^{-1}
Equiaxed volume fraction	0.36	0.23
Number density equiaxed dendrites	0.5 mm^{-3}	0.7 mm^{-3}

"LO"=lift-off

ACKNOWLEDGEMENTS

This work was financially supported by the German Space Agency DLR under grant no. 50 WM 0843, which is gratefully acknowledged. The authors appreciate the Team of Astrium Space Transportation GmbH in Trauen for the hardware development and support during the preparatory and final experiments. SSC, DLR-Moraba and Kayser-Threde are acknowledged for mission support at Esrange/Sweden.

REFERENCES

1. Pötschke M., Gaitzsch U., Roth S., Rellinghaus B., Schultz L., "Preparation of melt textured Ni–Mn–Ga", *J. Magnetism and Magnetic Materials,* Vol. 316(2), 383-385, 2007.
2. Wagner A., Shollock B.A., McLean M., "Grain structure development in directional solidification of nickel-base superalloys", *Mat. Sci. Eng. A*, Vol. 374(1-2), 270-279, 2004.
3. Martorano M.A., Beckermann C., Gandin Ch.-A., "A Solutal Interaction Mechanism for the Columnar to Equiaxed Transition in Alloy Solidification", *Met. Mat. Trans.*, Vol. 34A, 1657-1674, 2003.
4. Spittle J.A., "Columnar to equiaxed grain transition in as solidified alloys", *Int. Materials. Rev.*, Vol. 51, 247-269, 2006.
5. Mathiesen R.H., Arnberg L., "Stray crystal formation in Al–20 wt.% Cu studied by synchrotron X-ray video microscopy", *Mat. Sci. Eng.*, Vol. A 413–414, 283–287, 2005.
6. Witusiewicz V.T., Sturz L., Hecht U. and Rex S., "Thermodynamic description and unidirectional solidification of eutectic organic alloys: III. Binary systems neopentylglycol-(D)camphor and amino-methyl-propanediol-(D)camphor", *Acta Mat.*, Vol. 52 (19), 5519-5527, 2004.
7. Bayender et al., "Solid–liquid interfacial energy of camphene", *Mat. Sci. and Eng.*, Vol. A270, 343–348, 1998.
8. Ocak et al., "Solid–liquid interfacial energy of neopentylglycol", *J. Col. and Int. Sci.*, Vol. 320, 555–562, 2008.
9. Sturz L., Zimmermann G., Weiss A., "Transient Crystal Growth From Planar to Dendritic Interfaces Investigated during TEXUS-40", Proc. of the 17th ESA Symp. on European Rocket and Balloon Programmes and Related Research, Sandefjord, Norway, 30 May – 2 June (*ESA Sp-590*, August 2005).
10. Weiss A., Sturz L., Zimmermann G., "Investigation on the morphological instability during directional solidification of a transparent alloy during sounding rocket flights", *Mat. Sci. For.*, Vol. 508, 463-471, 2006.
11. Hunt J.D., "Steady State Columnar and Equiaxed Growth of Dendrites and Eutectic", *Mat. Sci. Eng.*, Vol. 65, 75-83, 1984.
12. Biscuola V.B. and Martorano M.A., „Mechanical Blocking Mechanism for the Columnar to Equiaxed Transition", *Met.and Mat. Trans. A*, Vol. 39A, 2885-2895, 2008.